Iraqi Journal of Science, 2026, Vol. 67, No. 1, pp: 240 -252
DOI: 10.24996/ijs.2025.67.1.19

ISSN: 0067-2904

Geological Interpretation of the Abu Jir Fault Zone between Hit and Kubaisa areas using a 2D Electrical resistivity imaging technique

Omama Talaat Rajab[1], Kamal Kareem Ali[1], Firas H. AL-Menshed[2]
[1]*Department of Geology, College of Science, University of Baghdad, Baghdad, Iraq*
[2] *General Commission for Groundwater, Ministry of Water Resource, Baghdad, Iraq*

Received: 6/10/2024 Accepted: 20/1/2025 Published: 30/1/2026

Abstract

The two-dimensional Electrical Resistivity Imaging (ERI) technique was used in this study to investigate The variations in resistivity within the Hit-Kubaisa area, Abu Jir Fault Zone (AJFZ) to detect fractures zone and evaluation of this technology in detecting faults. The study also aims to analyze the impact of these fractures on the geology of the region. Using the Wenner-Schlumberger array, the researchers conducted four survey lines with 120 electrodes spaced 10 meters apart, allowing them to map subsurface geological structures down to a depth of 240 meters. The results showed clear differences in resistivity, making identifying fracture zones and potential subsurface cavities possible. It also highlighted how these faults affect the sedimentary layers, especially the differences in the thickness of the Euphrates Formation and the absence of the Ana Formation.

Keywords: Abu Jir fault zone, 2D ERI technique, western Iraq, fracture detection, Wenner-Schlumberger array

التفسير الجيولوجي لنطاق صدع أبو جير بين منطقة هيت–كبيسة باستخدام تقنية تصوير المقاومية الكهربائية ثنائي الأبعاد.

امامه طلعت رجب[1]*, كمال كريم علي[1], فراس حميد المنشد[2]
[1]قسم الجيولوجيا, كلية العلوم, جامعة بغداد, بغداد, العراق
[2]الهيأة العامة للمياه الجوفية, وزارة الموارد المائية, بغداد, العراق

الخلاصة

تم تطبيق طريقة التصوير الكهربائي ثنائي الأبعاد (ERI) لدراسة تباينات المقاومة الكهربائية في منطقة هيت–كبيسة ولتحديد مناطق الكسور التحت سطحية ضمن نطاق فالق أبو جير (AJFZ). كما يقوم هذا البحث بتقييم فعالية تقنية ERI طريقة التصوير الكهربائي ثنائي الأبعاد في اكتشاف الفوالق والكسور. بالإضافة إلى ذلك، فإنه يبحث في تأثير هذه البُنى الجيولوجية على الجيولوجيا المحلية، وخصوصاً في الطبقات الرسوبية لتكويني الفرات والدمام. تم إجراء أربع خطوط مسح باستخدام ترتيب Wenner–Schlumberger ، حيث تم توزيع 120 قطباً كهربائياً على مسافات متباعدة بمقدار 10 أمتار. وقد نجحت هذه الطريقة في رسم التراكيب الجيولوجية التحت سطحية وصولاً إلى عمق 240 متراً. وأظهرت النتائج تباينات كبيرة في المقاومة الكهربائية، مما أتاح تحديد مناطق الكسور والتجاويف المحتملة تحت السطح. كما

*Email: omame.rajab2308@sc.uobaghdad.edu.iq

أبرزت النتائج تأثير الفوالق على سمك التكوينات الرسوبية، مما يؤكد دورها في تشكيل الخصائص الجيولوجية للمنطقة.

Introduction

Electrical Resistivity Imaging (ERI) is a valuable method for detecting fracture zones and other geological features by measuring subsurface variations in resistivity. Faults often exhibit distinct resistivity contrasts due to differences in lithology, fluid content, and fracturing [1, 2]. Electric resistivity imaging (ERI) has been effectively utilized in Iraq for various subsurface investigations across multiple fields. It is commonly used to identify weak subsurface zones, detect buried archaeological artefacts, locate water leaks, characterize underground reservoirs, [3-7] In the western desert, karst phenomena are common, with 3D resistivity imaging revealing numerous small cavities at various depths [8, 9].

The ERI method has been applied in various tectonic environments. For instance, in the Karachi Arc in Pakistan, ERI has proven useful in identifying active fault zones by revealing distinct resistivity contrasts between faulted and unfaulted rock masses [10]. In western Argentina, this technique was used to characterize Quaternary faults.[11]. In Egypt's Eastern Desert, ERI played a crucial role in mapping fault zones [12]. In Iraq , the 2D ERI technique was applied to study fractures subsurface in the Abu Jir Fault Zone area southwest of Karbala, where the imaging results revealed two distinct types of fracture zones [13].

The existence of the AJFZ has caused a complex interplay between radioactivity, groundwater quality, oil seepage, and structural geology, all shaped by the fault system [14-16]. Detecting near-surface faults is required for a deeper understanding of the geological conditions of the area.

The primary goal of this study is to accurately identify the locations of faults and fractures in the Hit-Kubaisa area using the two-dimensional resistivity imaging method. This research will also assess how effectively this technique detects such features. Additionally, the study will analyze the effect of these faults and fractures on the geological structures, particularly in the sedimentary layers of the Euphrates and Dammam formations.

Study Area and the Geological Setting

The study area is located in the AJFZ area between Hit and Kubaisa within Anbar Governorate, western Iraq (Figure 1).

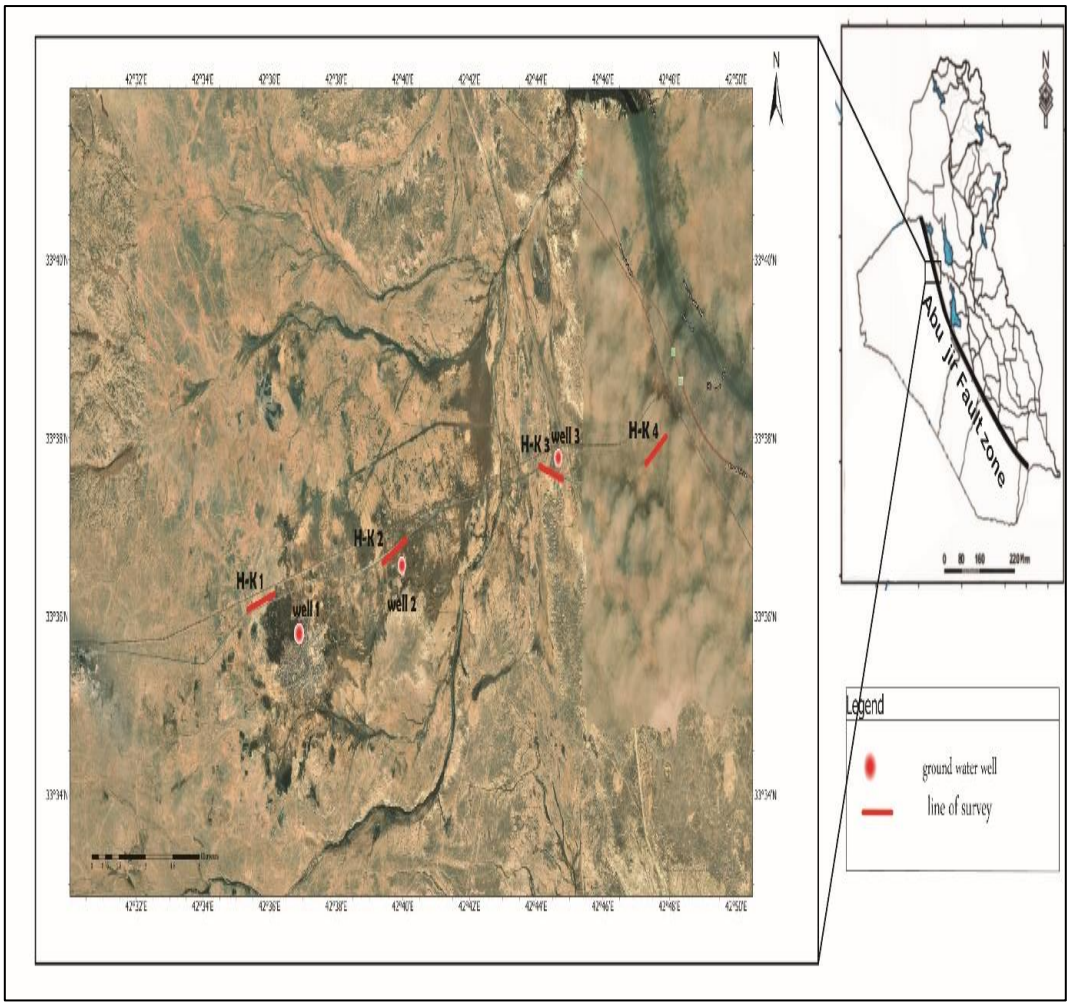

Figure 1: Locations of the 2D resistivity survey lines in the study area.

The surface geology of the study area and near it is found that near Hit City Fatha Formation consists of gypsum, layered limestone, and green marl, with a thickness of around 20 meters, while near Kubaisa, the Euphrates Formation is exposed. The region also contains Quaternary sediments, including valley fill, residual soil, and gypcrete deposits [17] (Figure 2).

(Figure 3) shows the stratigraphic column of three wells drilled in the study area by the General Commission of Groundwater [18].

Listed as the oldest, the Dammam Formation (Middle Eocene) consists of limestone and dolomitic limestone. Ana Formation (Oligocene) consists of limestone that is about 15 meters thick. Euphrates Formation (Miocene) consists of well-layered recrystallized limestone and chalky limestone, with thicknesses ranging from 30 to 50 meters, deposited in a shallow marine environment rich in fossils.

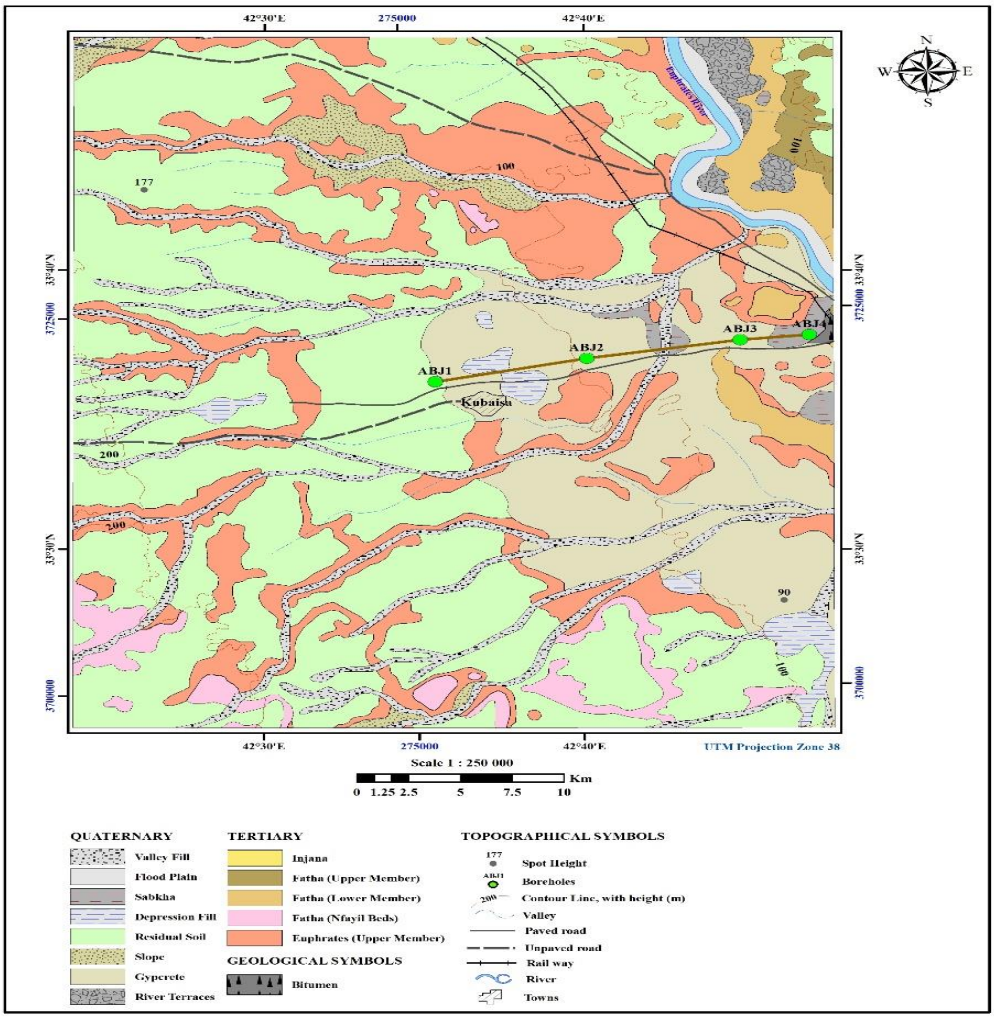

Figure 2: Geologic map of the study area [17].

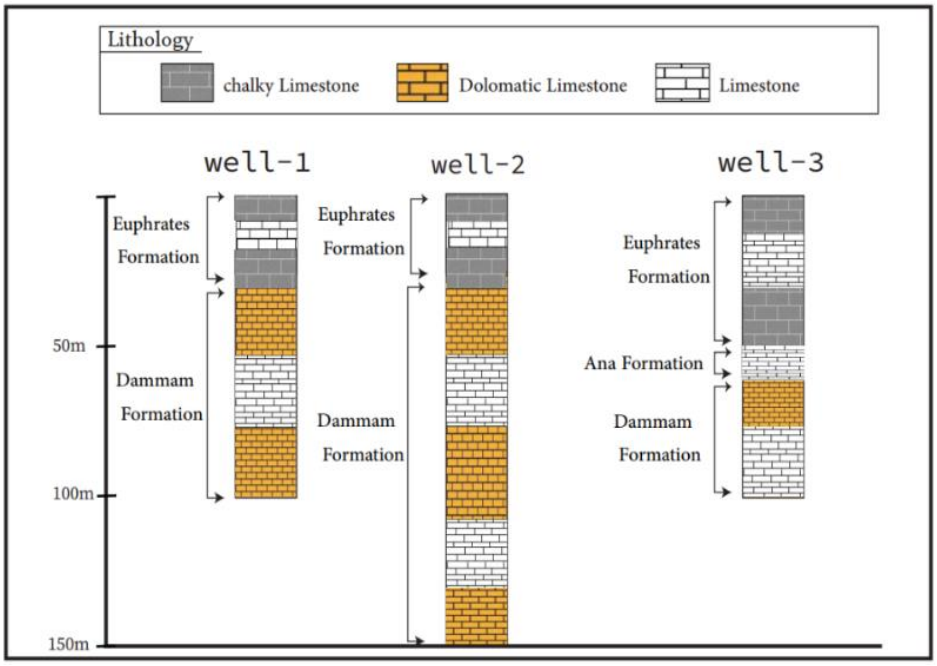

Figure 3: Subsurface lithological setting in the study area [18]

Tectonically, the area is located within the Arabian Platform, situated between the Mesopotamian sub-region and the Western Desert sub-region, which is divided by the Ana-Abu Jir-Euphrates fault system[19] (Figure 4). The AJFZ is a major geological structure in western Iraq that influences the tectonic landscape of the region. The AJFZ exhibited characteristics of a right-lateral strike-slip fault [20]. The region's structure is further highlighted in seismic sections by the presence of positive and negative tectonic features. The southern part forms depressions due to the negative veneer structure, while the northern part forms successive hills and slopes [21].

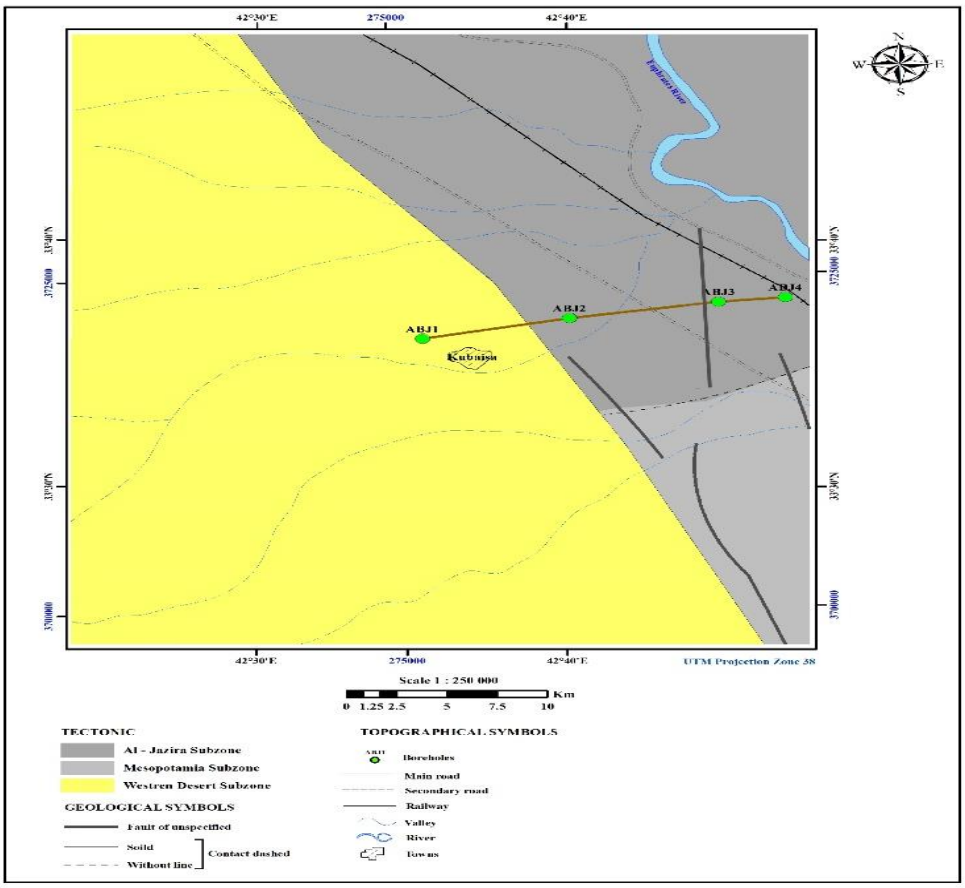

Figure 4: Structural map of the study area [19]

Cavities in western Iraq are primarily formed due to karst processes, which are prevalent in regions with soluble carbonate rocks like limestone and dolomite. These processes result from the dissolution of these rocks by slightly acidic rainfall or groundwater, creating underground voids, sinkholes, and cavities. In Iraq's western desert, especially within the Euphrates Formation (Lower Miocene), significant karst features such as sinkholes and subsurface cavities are common [22, 23].

Oil seepage is found in the Abu Jir Fault Zone in western Iraq, resulting from tectonic activity that facilitates the migration of hydrocarbons from deep rocks to the surface. These seepages are associated with the Fatha and Euphrates formations [24, 25].

Data acquisition and processing

Before starting fieldwork, ElectreII Pro software was used to optimize the survey parameters including electrode spacing (a-spacing), the n-factor, the total length of the traverse, the number of electrodes, and the depth of investigation.

The Syscal Pro Switch 120 multielectrode resistivity meter was used for data acquisition. This system, which has 120 electrodes, was used to complete four 2D resistivity survey lines.

Each line was 1,190 meters long, with electrodes spacing 10 meters. The n-factor ranged from 1a to 6a, with an expected maximum depth of investigation of 246.9 meters.

Wenner-Schlumberger electrodes configuration was used because it has several advantages, making it a common arrangement to have a good balance between horizontal resolution and depth of investigation. Locations of the survey lines were chosen carefully to cross the strike of main features in the area, especially the AJFZ. The geographic coordinates of the first and last electrodes are detailed in Table 1, and their locations are shown in (Figure 1).

RES2DINV software was used for data inversion. The finite-element method was applied for forward modelling because survey lines contain topographic variations. For data inversion, the robust least squares were used because it is better suited for detecting sharp boundaries of subsurface structures and can give a model with less ABS error per cent[1].

Table 1: the coordinates of the 2D resistivity lines within the study area.

Line name	First electrode longitude and latitude	Last electrode longitude and latitude	Direction of survey	Elevation in m (ASL.)
H-K1	E 42° 35' 20" N 33° 36' 02"	E 42° 36' 06" N 33° 36' 10"	N 75° E	134
H-K2	E 42° 39' 21" N 33° 36' 39"	E 42° 40' 07" N 33° 36' 52"	N 67.5° E	96
H-K3	E 42° 44' 05" N 33° 37' 39"	E 42° 44' 55" N 33° 37' 32"	S 75° E	83
H-K4	E 42° 47' 04" N 33° 37' 41"	E 42° 47' 47" N 33° 38' 01"	N 60° E	65

Results and Discussion

The first geoelectric zone in the section exhibits resistivity values ranging from 11 to 15 Ω m, at a depth of 30 to 40 m, the inverse model of section H-K1 (Figure 5) shows that this contact, marked by a black line, extends throughout the section, which is in good agreement with the expected resistivity of the limestone and chalky limestone of the Euphrates Formation. It also corresponds to the depth of the Euphrates Formation according to the well-1 data indicating that the contact between the Euphrates and Dammam formations is located at a depth of about 30 m (Figure 3).

Several anomalies with high and low resistivity values are also present in this zone. High resistivity anomalies are observed at depths of 5 to 25 m and extend over intervals of 160 to 200 m, 300 to 340 m, 620 to 680 m, and 940 to 980 m, with resistivity values ranging from 100 to 108 Ω m. These anomalies are likely indicative of subsurface cavities, possibly formed due to the dissolution of carbonate rocks by infiltration of rainwater along fractures and fissures. These cavities may also contain bituminous materials. Low resistivity anomalies are identified at a depth of about 60 m, covering intervals of 150–190 m, 320–360 m, 640–680 m, and 950–990 m from the start of the section, with resistivity values ranging from 2 to 6 Ω m. These are likely indicative of eroded zones, fractures, or water-filled voids.

The second geoelectric zone is located at a depth of less than 60 m, where resistivity values range from 70 to 120 Ω m; this increase in values reflects the transition to a different geological unit where it corresponds to Dammam Formation represented by limestone and dolomitic limestone.

In this zone, lateral variations in resistivity values ranging from 70 to 120 Ω m were observed. This variation may indicate the presence of fracture zones containing fluids, which likely contributed to the reduction in resistivity values.

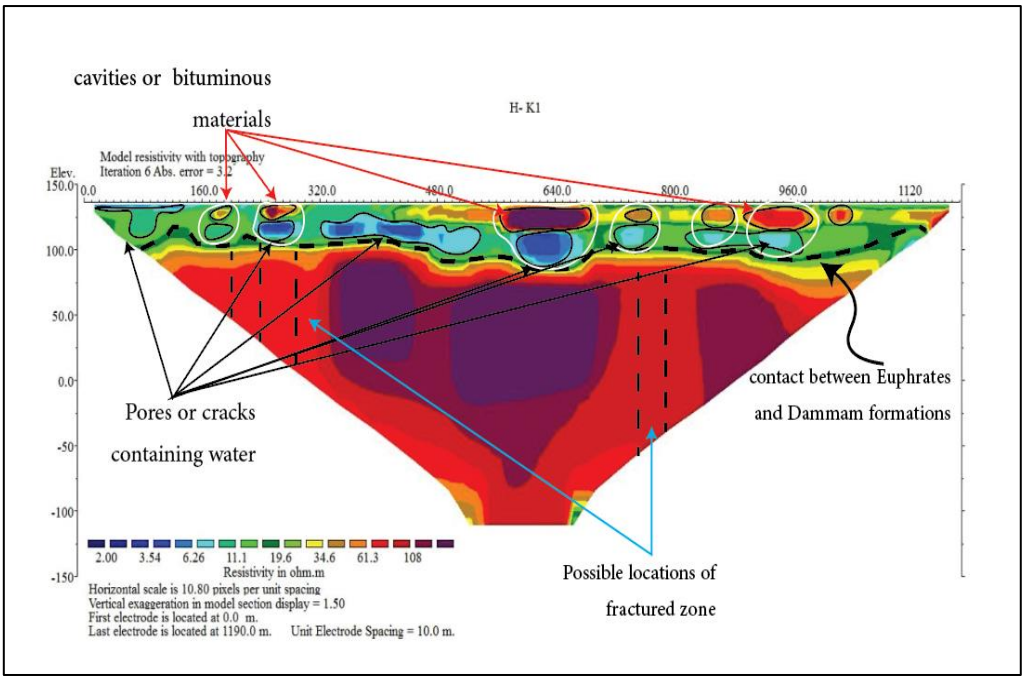

Figure 5: Inverted model of 2D resistivity for H-K1

According to well-2 near the H-K2 section, the depth of the contact between the Euphrates and Dammam formations is approximately 30m (Figure 3).

In the inverted model of section H-K2 (Figure 6) it is found that the first geoelectric zone extends along the section and its depth varies between (30 – 33) m, with resistivity values ranging from 2 to 6 Ωm which is approximately consistent with the depth of this contact according to well-2 near the H-K2 section, the depth of the contact between the Euphrates and Dammam formations is approximately 30m (Figure 3).
The cause of low resistivity in the first geoelectric zone is the presence of water in the pores or fractures, which causes a decrease in the resistivity values.

In the second geoelectric zone, a significant lateral variation in resistivity values is observed between 350 and 650 meters from the start of the section at depths ranging from approximately 75 to 150 meters. This variation in resistivity may indicate the presence of a fractured zone, which caused a decrease in resistivity values at the location of these fractures, as illustrated in (Figure 6). This interpretation has coincided with a geological survey report [26] where the survey line is cut by a residual gravity anomaly, marked Gr1. Gravity markers Grl could express shallow fault (Figure 7).

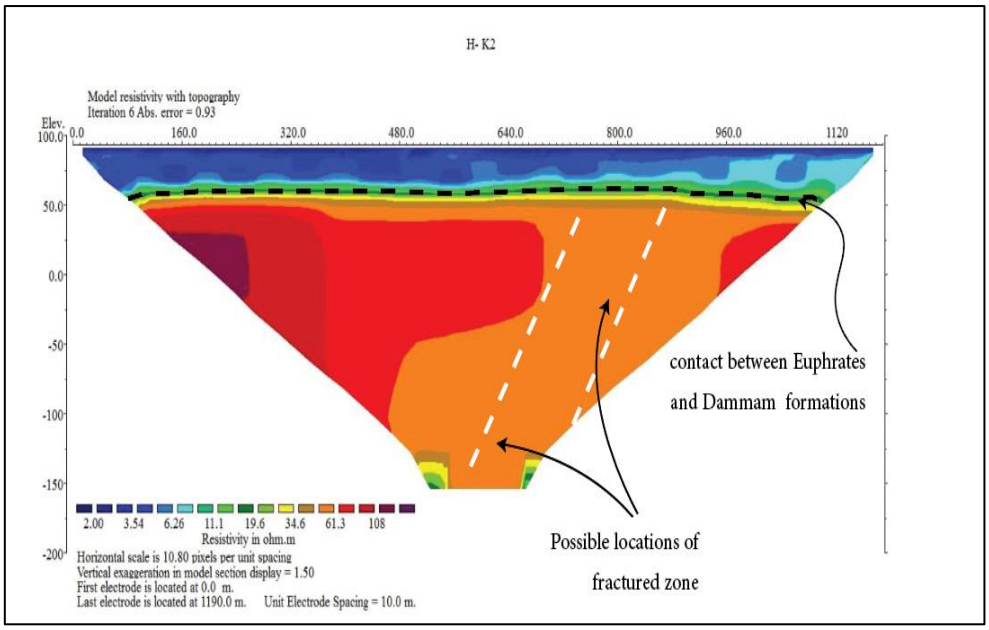

Figure 6: Inverted model of 2D resistivity for H-K**2**

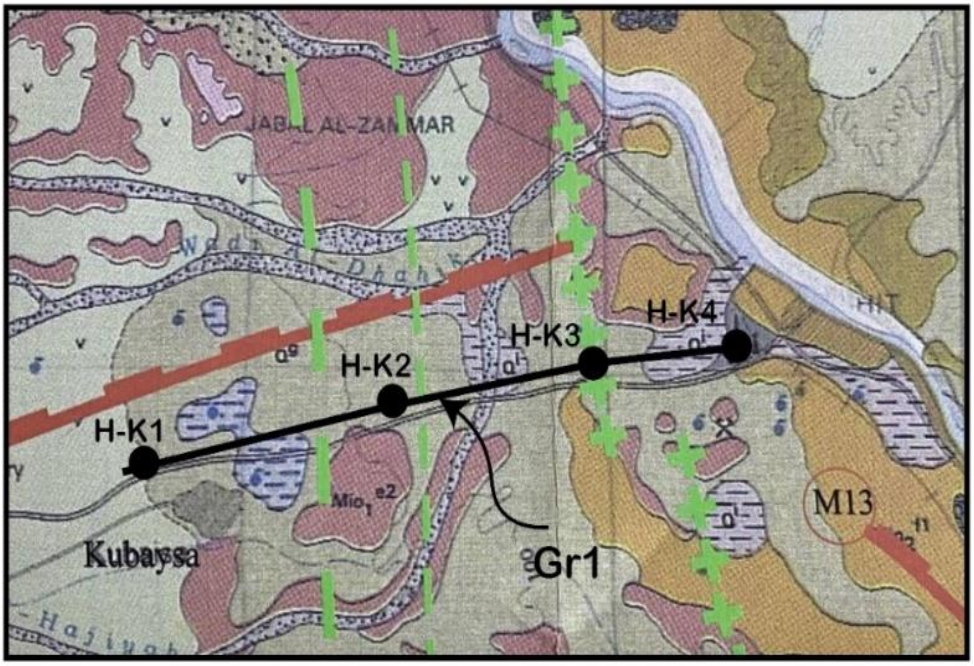

Figure 7: Location of an anomaly (Gr1) extracted by gravity measurements survey (After permission of Geosurv) [26].

In the reverted model of the H-K3 section (Figure 8), the first geoelectric zone appears at a depth ranging from (50 – 125m) with resistivity values ranging from 11 to 15 Ω m. These values are consistent with the resistivity values of the Euphrates Formation, which consists of limestone and chalky limestone. The contact depth between the Euphrates and Ana Formations is about 50m according to well-3 near the H-K3 section (Figure 3). Some anomalies with low and high values are also shown in this zone.

The second geoelectrical zone shows a lateral variation in resistivity values ranging from 30 to 70 Ωm. This variation indicates the presence of a fault according to the structural map of the area which indicates the presence of a fault perpendicular to the survey line (Figure 4).

The wide variation in the thickness of the Euphrates Formation could be due to the displacement at the fault plane.

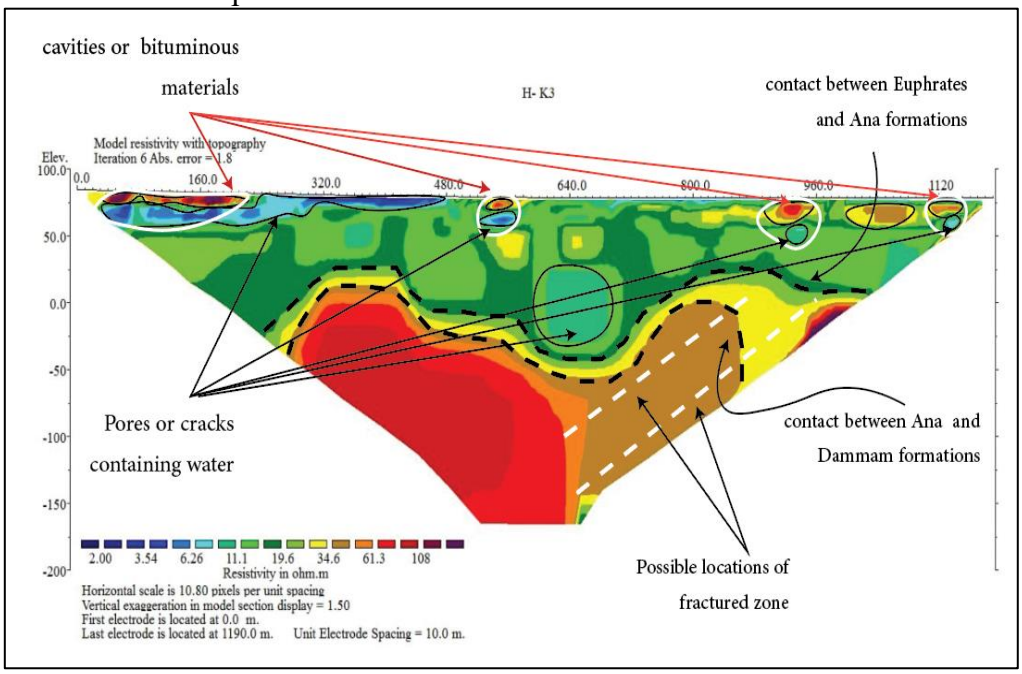

Figure 8: Inverted model of 2D resistivity for H-K3

In the inverted model of section H-K4 in figure 9, it is found that the thickness of the first geoelectric zone was (75) m with resistivity values ranging from 11 to 15 Ωm, this zone is considered to represent the Euphrates Formation. The contact between the Euphrates and underneath the Ana Formation delineated as a (black dashed line) extends along the section. At a depth of approximately 5 m, several anomalies appear with high resistivity values ranging from 34.6-108 Ωm, indicating the presence of cavities that may contain bituminous materials. From a depth of 20 to a depth of 70, an area appears with resistance values of 5-6 Ωm, which indicates the presence of water in the pores or fractures.

The second electric zone in this section appears with resistance values ranging from 20 to 30 Ω m, and depth between 75 to 90 m, about 15 m thickness. This is consistent with the resistivity values of the limestone forming the Ana Formation and the thickness of the Ana Formation apparent in Well-3 (Figure 3).

The third geoelectric zone appears below 90 m depth with resistivity values ranging from 70 to 120 Ωm. This zone represents limestone and dolomite limestone of the Dammam Formation, according to the information from well 3.
In this zone, lateral variations in resistivity values ranging from 70 to 108 Ω m were observed. This variation may indicate the presence of fractures or fault zones containing water, which likely contributed to the reduction in resistivity values.

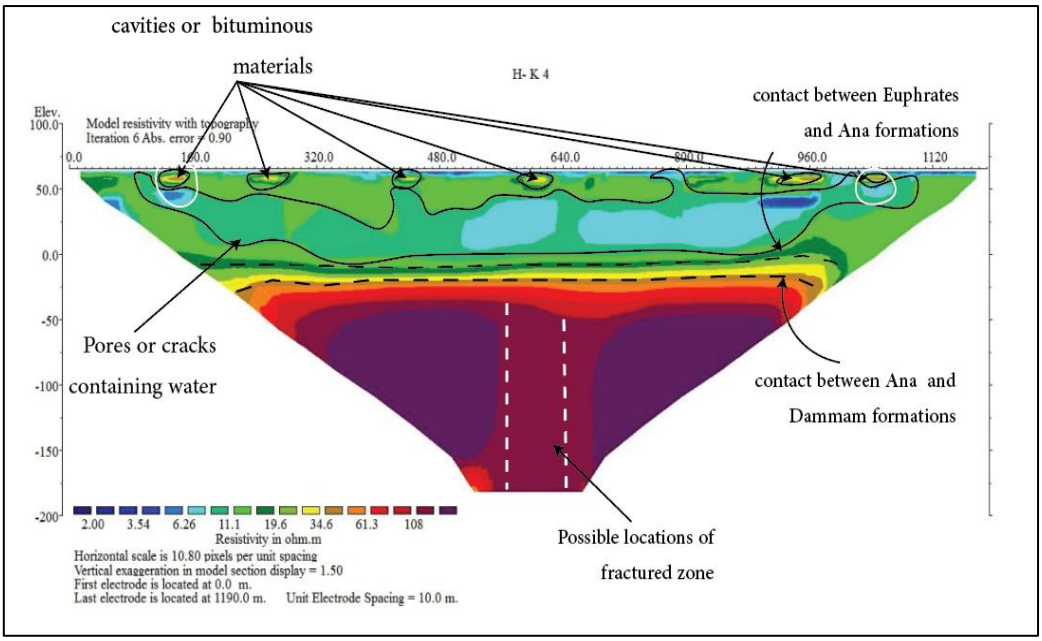

Figure 9: Inverted model of 2D resistivity for H-K4

In the Euphrates Formation of the resistivity sections, a repeated anomaly pattern is observed, as indicated by the white circles. This pattern consists of very high resistivity anomalies in the uppermost layer, immediately followed by very low resistivity anomalies beneath them. These features are consistent with a phenomenon identified south of the study area and extending perpendicular to the survey lines (Figure 10), where buried channels exhibit air-filled cavities near the surface, with water-saturated zones underneath. This explains the presence of subsurface voids, possibly related to karst processes or collapsed features, filled with air and water.

Figure 10: shows the buried channels on the surface near survey line H-K1 and their location on the map of the area.

A geological cross-section of the study area, based on groundwater well data (Figure 11), was compared with a section derived from Electrical Resistivity Imaging (ERI) data (Figure 12). Both sections reveal a similar structural framework, particularly showing an increase in the thickness of the Euphrates Formation and the absence of the Ana and Fatha formations, which can be attributed to the presence of faults in the area.

The Fatha Formation only appears as an outcrop in Hit city near the section H-K4, it does not appear further toward Kubaisa city Fatha Formation is absent in the nearby wells within the study area. It has also not been observed or identified in the inverted section H-K4.
In the H-K2 inverted section, there is no Anna Formation. In the H-K3 inverted section, there is a significant thickening of the Euphrates Formation. These differences in the layers are likely due to the influence of faults in both sections, indicating that these faults played a major role in shaping the geology of the area. The fault in the H-K3 section could be responsible for the disruption of the Anna Formation.

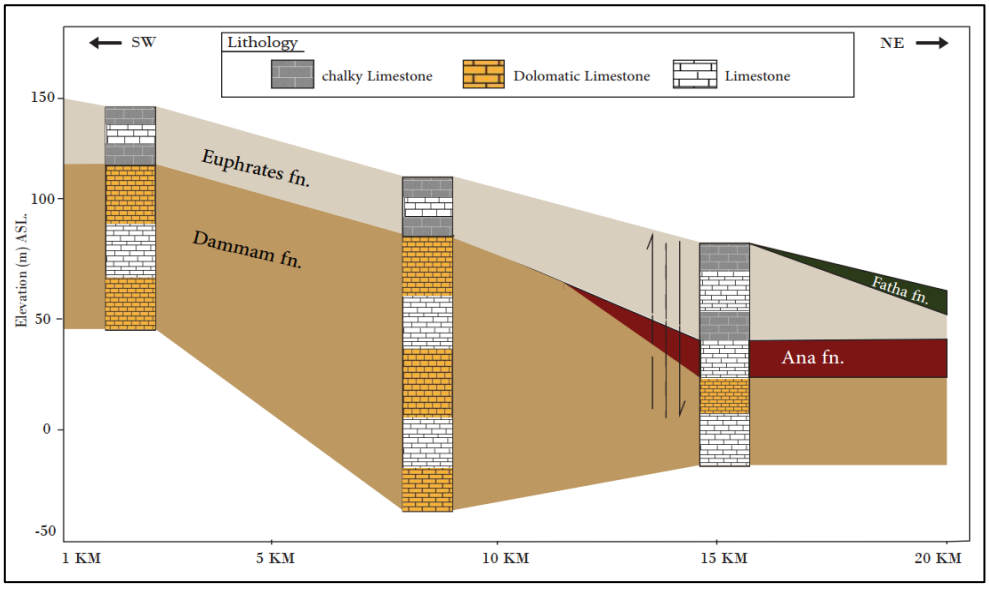

Figure 11: Geological cross-section of the study area, based on groundwater well data, shows the fault based on a structural map.

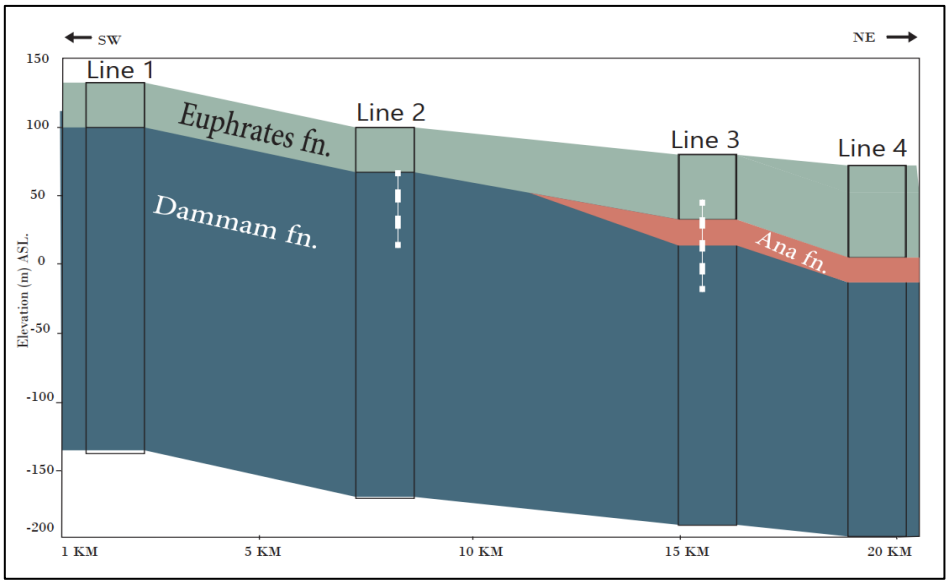

Figure 12: Geological cross-section derived from Electrical Resistivity Imaging (ERI) data.

Conclusion:

This study shows that 2D electrical resistivity imaging (ERI) is an effective tool for detecting faults and fractures in the Hit-Kubaisa area of western Iraq, especially within the Abu Jir fault zone. By identifying resistivity variations across geological layers, the resistance values within the fracture zone from 40 to 70 Ωm, as the fractures allow the presence of fluids, which results in a decrease in resistance values. The study successfully identifies potential fault locations and subsurface cavities that may contain fluids or bituminous materials.

The results also reveal how these faults affect sedimentary strata, particularly in the thickness variations of the Euphrates Formation and the absence of Ana and Fatha formations at certain locations. These observations indicate that faults significantly influence the geological features of the area.

References

[1] M. H. Loke, I. Acworth, and T. Dahlin, "A comparison of smooth and blocky inversion methods in 2D electrical imaging surveys," *Exploration geophysics,* vol. 34, no. 3, pp. 182-187, 2003.

[2] J. M. Reynolds, *An introduction to applied and environmental geophysics*. John Wiley & Sons, 2011.

[3] N. A. Alrawi and T. T. Al-Samarrai, "Determine Water Level by Electrical Resistivity and Comparing Results with Drilled Well in Al-Naharwan, Baghdad," *The Iraqi Geological Journal,* pp. 301-313, 2023.

[4] F. Z. Berhi and O. S. Al-Saadi, "Electrical Resistivity Synthetic Modeling and Field Survey for Subsurface Features Investigation of the Borsippa Archaeological Site, Babylon Governorate, Middle Iraq," *The Iraqi Geological Journal,* pp. 33-46, 2024.

[5] M. A. Noon, A. M. Abed, and F. H. Al-Menshed, "Groundwater Investigation Using Electrical Resistivity Imaging Technique in Western Ramadi, Iraq," *The Iraqi Geological Journal,* pp. 139-145, 2023.

[6] A. M. Salman and A. M. Al-Rahim, "Integrated Geophysical Methods to Discriminate the Locations of the Subsurface Weakness Zone Areas in the State Company for Glass and Refractories at Al-Ramadi City, Iraq," *The Iraqi Geological Journal,* pp. 266-274, 2024.

[7] W. D. AL-Mahemmdi, A. S. Al-Banna, and F. H. AL-Menshed, "Detection of A Possible Subsurface Water Seepage Using 2D Electrical Resistivity Imaging Survey at a site in Al-Khwarizmi College of Engineering, University of Baghdad, Iraq," *Iraqi Journal of Science,* pp. 1810-1819, 2023.

[8] O. H. Al-Jumaily, A. M. Abed, and K. K. Ali, "Using 2D Resistivity Imaging Technique to Detect and Delineate Shallow Unknown Cavities In Al-Haqlaniyah Area, Western Iraq," *Iraqi Journal of Science,* pp. 1091-1102, 2022.

[9] O. H. Al-Jumaily, A. M. Abed, and K. K. Ali, "Detection of Shallow Cavities Using 3D Resistivity Technique in a Small Site Near Haditha City, Western Iraq," *Iraqi Journal of Science,* pp. 1557-1564, 2022.

[10] A. Nabi, X. Liu, Z. Gong, and A. Ali, "Electrical resistivity imaging of active faults in palaeoseismology: case studies from Karachi Arc, southern Kirthar Fold Belt, Pakistan," *NRIAG Journal of Astronomy and Geophysics,* vol. 9, no. 1, pp. 116-128, 2020.

[11] S. Y. Fazzito, A. E. Rapalini, J. M. Cortés, and C. M. Terrizzano, "Characterization of Quaternary faults by electric resistivity tomography in the Andean Precordillera of Western Argentina," *Journal of South American Earth Sciences,* vol. 28, no. 3, pp. 217-228, 2009.

[12] A. Ammar and K. Kamal, "Resistivity method contribution in determining of fault zone and hydro-geophysical characteristics of carbonate aquifer, eastern desert, Egypt," *Applied water science,* vol. 8, pp. 1-27, 2018.

[13] A. S. Al-Zubedi and J. M. Thabit, "Use of 2D azimuthal resistivity imaging in delineation of the fracture characteristics in Dammam aquifer within and out of Abu-Jir fault zone, central Iraq," *Arabian Journal of Geosciences,* vol. 9, no. 1, p. 22, 2016.

[14] B. M. Hussien and M. A. Gharbi, "HYDROGEOLOGICAL CONDITIONS WITHIN ABU-JIR FAULT ZONE (HIT–KUBAIYSA)," 2010.
[15] O. J. Mohammed, A. M. Abed, and M. A. Alnuaimi, "Evaluation and delineation of sulfur groundwater leakages using electrical resistivity techniques in Hit Area, Western Iraq," *Iraqi Journal of Science,* pp. 2239-2249, 2021.
[16] K. K. Ali, "The geological situation in Abu-Jir Faults Zone, western Iraq: evidence from the radioactivity in Hit–Haditha area," *Environmental Earth Sciences,* vol. 82, no. 10, p. 241, 2023.
[17] S. Jassim and J. Goff, "Geology of Iraq: DOLIN, sro, distributed by Geological Society of London," ed, 2006.
[18] General Commission of Groundwater,"*report groundwater well*" , npublish, 2014.
[19] S. F. Fouad, "Tectonic map of Iraq, scale 1: 1000 000, 2012," *Iraqi Bulletin of Geology and Mining,*vol. 11, no. 1, pp. 1-7, 2015.
[20] S. F. Fouad, "Contribution to the structure of Abu Jir fault zone, west Iraq," *Iraqi Geological Journal,* vol. 32, no. 1991–2000, pp. 63-73, 2004.
[21] L. R. Alkhafaji and A. A. Alhadithi, "Variable behaviour of Abu Jir fault zone, western Iraq," in *IOP Conference Series: Earth and Environmental Science*, 2024, vol. 1300, no. 1: IOP Publishing, p. 012043.
[22] S. O. Al-Hetty, N. Z. Al-Salmani, and O. J. Mohammad, "Comparison of the Manifestations of Western Region-Iraq Karst and Some Typical Karst Areas in the World," in *IOP Conference Series: Earth and Environmental Science*, 2022, vol. 1080, no. 1: IOP Publishing, p. 012016.
[23] V. K. Sissakian1, N. A.-A. , and a. S. Knutsson3, "Karst Forms in Iraq," *Journal of Earth Sciences and Geotechnical Engineering,* vol. vol. 5, no.4, , , pp. 1-26, 2015.
[24] M. W. Alkhafaji *et al.*, "Organic geochemistry of hydrocarbon seeps associated with sulfurous spring water, western Iraq: Biodegradation, source rock and sedimentary environment," *Journal of Petroleum Science and Engineering,* vol. 208, p. 109556, 2022.
[25] A. J. Al-Khafaji, M. H. Hakimi, E.-K. Ibrahim, A. A. Najaf, H. Al Faifi, and A. Lashin, "Organic geochemistry of oil seeps from the Abu-Jir Fault Zone in the Al-Anbar Governorate, western Iraq: Implications for early-mature sulfur-rich source rock," *Journal of Petroleum Science and Engineering,* vol. 184, p. 106584, 2020.
[26] J. M. A. Al-bdaiwi, "structural markers infered from geophysical data," Geoserv report unpublished, 2009.